

Radiation-reaction force on a particle plunging into a black hole

Leor Barack

Department of Physics, Technion—Israel Institute of Technology, 32000 Haifa, Israel

Lior M. Burko

Theoretical Astrophysics, California Institute of Technology, Pasadena, California 91125

(October 29, 2018)

We calculate the self force acting on a scalar particle which is falling radially into a Schwarzschild black hole. We treat the particle's self-field as a linear perturbation over the fixed Schwarzschild background. The force is calculated by numerically solving the appropriate wave equation for each mode of the field in the time domain, calculating its contribution to the self force, and summing over all modes using Ori's mode-sum regularization prescription. The radial component of the force is attractive at large distances, and becomes repulsive as the particle approaches the event horizon.

PACS number(s): 04.25-g, 04.70.-s, 04.70.Bw

The problem of finding the equations of motion for a particle in curved spacetime is a long-standing open problem in General Relativity. Recently, this problem has also become timely and extremely important. The planned Laser Interferometer Space Antenna (LISA) is expected to detect (among other sources) the gravitational waves emitted from a compact object orbiting a supermassive black hole (BH). Accurate templates, which include also the radiation-reaction (RR) effects on the compact-object's orbit, are essential for the detection of the signal.

The traditional approach for calculation of the orbital evolution under RR requires the calculation of the fluxes at infinity and through the BH's event horizon (EH), of quantities which are constants of motion in the absence of RR. Then one uses balance arguments to relate these fluxes to the local quantities of the object [1]. However, such techniques typically fail, because the evolution of the Carter constant, which is a non-additive constant of motion, cannot be found by balance arguments [2].

Several prescriptions to include the RR effects in the orbital evolution have been suggested. Quinn and Wald [3] and Mino, Sasaki, and Tanaka [4] recently proposed general approaches for the calculation of self forces. However, it is not clear how to practically apply these approaches for actual computations, the greatest problem being the calculation of the non-local "tail" contribution to the self force, which arises from the failure of the Huygens principle in curved spacetime. More recently, Ori proposed a practical approach for the calculation of the self force [5,6], which is based on decomposition of the self force into modes, and on a mode-sum regularization prescription (MSRP). MSRP has been developed in full in Refs. [7,8] for a scalar particle in static spherically-symmetric spacetimes, and has been applied for several non-trivial cases including a static scalar charge outside a Schwarzschild black hole (SBH) [9] and a scalar charge in circular orbit around a SBH [10]. In addition, there is strong evidence that MSRP is applicable also for electric-

field RR [9,11], and some evidence that it is applicable also for gravitational-field RR [12].

MSRP has been directly applied until now only for stationary problems, where the field was decomposed into Fourier-harmonic modes, and the analysis was done in the frequency domain. This was easy to be done in [10] for the case of circular orbits around a SBH, because the RR in that case admits a discrete spectrum. However, in general one faces a time-dependent, evolutionary problem, and one expects the spectrum to be continuous rather than discrete. In this paper, we apply MSRP for the first time to a time-dependent, dynamical problem.

We consider a pointlike massless particle of scalar charge q , moving along a radial (timelike) geodesic outside a SBH of mass $M \gg |q|$, where the metric is $ds^2 = -F(r) dt^2 + F^{-1}(r) dr^2 + r^2 d\Omega^2$, $d\Omega^2$ being the metric on the unit 2-sphere, and $F(r) = 1 - 2M/r$. Let the particle's worldline be represented by $x^\mu = x_p^\mu(\tau)$, with τ being the proper time along the geodesic. For inward radial geodesic motion, to be considered here, we have (in Schwarzschild coordinates) $\dot{\theta}_p = \dot{\varphi}_p = 0$,

$$\dot{r}_p = -[E^2 - F(r_p)]^{1/2}, \quad \text{and} \quad \dot{t}_p = E/F(r_p), \quad (1)$$

where a dot denotes $d/d\tau$, and E is the energy parameter (which is a constant of motion in the absence of the self force). The scalar field Φ coupled to the particle satisfies the inhomogeneous wave equation

$$\square\Phi = -4\pi q \int_{-\infty}^{\infty} \delta^4[x^\mu - x_p^\mu(\tau)] (-g)^{-1/2} d\tau, \quad (2)$$

g being the metric determinant, and \square denoting the covariant wave operator. We next decompose Φ into modes

$$\Phi = \sum_{\ell=0}^{\infty} \phi^\ell = 2\pi q \sum_{\ell,m} Y_{\ell m}(\theta, \varphi) \left[Y_{\ell m}^*(\theta_p, \varphi_p) \frac{\psi^\ell}{r} \right], \quad (3)$$

where $Y_{\ell m}(\theta, \varphi)$ are the standard scalar spherical harmonics, an asterisk denotes complex conjugation,

and $\psi^\ell = \psi^\ell(r, t; r_p, t_p)$. By expanding the delta function in Eq. (2) as $\delta(\theta - \theta_p)\delta(\varphi - \varphi_p) = \sum_{\ell, m} \sin\theta Y_{\ell m}(\theta, \varphi) Y_{\ell m}^*(\theta_p, \varphi_p)$ and using the orthogonality of the $Y_{\ell m}$, we find that ψ^ℓ satisfies

$$\psi_{,uv}^\ell + V^\ell(r)\psi^\ell = S(r; r_p). \quad (4)$$

Here, $v \equiv t + r^*$ and $u \equiv t - r^*$ (with $r^* \equiv r + 2M \ln[(r - 2M)/2M]$) are the ingoing and outgoing Eddington null coordinates, correspondingly, the effective potential is given by $V^\ell(r) = (F/4) [\ell(\ell + 1)r^{-2} + 2Mr^{-3}]$, and

$$S \equiv \frac{F}{2r} \int_{-\infty}^{\infty} \delta(r - r_p) \delta(t - t_p) d\tau = \frac{F^2}{2rE} \delta(r - r_p). \quad (5)$$

[In the last equality we use $d\tau = dt/\dot{t} = (F/E)dt$, followed by integration over t .] Finally, we express the modes ϕ^ℓ in terms of the (m -independent) functions ψ^ℓ by summing over the azimuthal numbers m in Eq. (3). For radial motion we thus find that

$$\phi^\ell = q \left(\ell + \frac{1}{2} \right) \frac{\psi^\ell}{r}. \quad (6)$$

The *total* regularized self force (including both the local and the tail parts) exerted on the scalar particle, f_α^{RR} , can be calculated by [7,8,13]

$$f_\alpha^{\text{RR}} \equiv \sum_{\ell=0}^{\infty} \left[f_\alpha^{\ell \pm} - A_\alpha^\pm \left(\ell + \frac{1}{2} \right) - B_\alpha \right] \quad (7)$$

(evaluated on the particle's worldline), where $f_\alpha^\ell = q\phi_{,\alpha}^\ell$ is the (covariant) self-force contribution associated with the ℓ -mode of the particle's self-field, and A_α^\pm and B_α are regularization parameters, whose values are given by Eqs. (101) and (134) of Ref. [8]. For the radial geodesics considered here, these parameters take the form

$$A_{r^*}^\pm = \mp \frac{q^2}{r^2} E, \quad A_t^\pm = \pm \frac{q^2}{r^2} \dot{r}, \quad (8)$$

$$B_{r^*} = -\frac{q^2}{2r^2} (2F - E^2), \quad B_t = -\frac{q^2}{2r^2} \dot{r} E \quad (9)$$

(with all quantities evaluated at $x^\mu = x_p^\mu$). One should use $f_\alpha^{\ell+}$, A_α^+ ($f_\alpha^{\ell-}$, A_α^-) when one calculates the field's gradient from the $r \rightarrow r_p^+$ ($r \rightarrow r_p^-$) limit (in general $f_\alpha^{\ell+} \neq f_\alpha^{\ell-}$ [7,8]). (Of course, the physical quantity f_α^{RR} can be derived from either of these two values, or from any of their linear combinations.) In practice, we take below the $r \rightarrow r_p^-$ limit.

Thus, in practice, to derive the self force along any given radial geodesic (parametrized by E), one should first solve Eq. (4) for the various modes (with appropriately chosen initial data—see below), then construct the quantities f_α^ℓ , and finally sum over the regularized self-force modes using Eq. (7). This sum over modes is

expected to converge at least as $1/\ell$, as the $O(1/\ell)$ term in the $1/\ell$ expansion of f_α^ℓ vanishes [7,8].

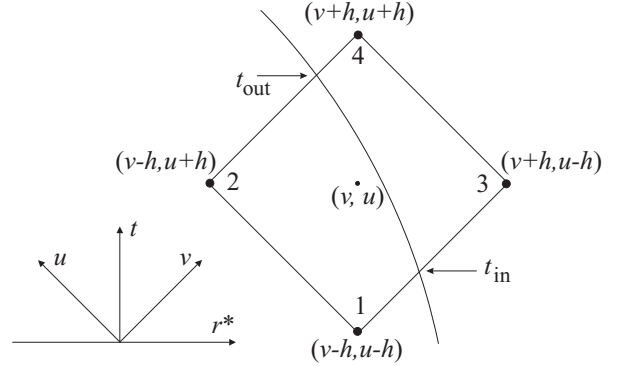


FIG. 1. Numerical grid cell containing a section of the worldline. (See the text for further explanation.)

To solve for ψ^ℓ , we integrate Eq. (4) numerically (in the time domain) on a double-null grid. This grid is spanned by v and u , covering the entire exterior of the SBH (with the EH approached at $u \rightarrow \infty$). A characteristic initial-value problem for ψ^ℓ is set up by specifying initial data on two null hypersurfaces $v = v_0$ and $u = u_0$, taken to intersect at some point along the particle's worldline. As initial data we take the exact solution corresponding to a static particle held fixed at $r_0^* \equiv (v_0 - u_0)/2$ [9]. This solution is not the actual initial field of the geodesic particle considered here (which is unknown, in general). However, it does approximate the initial field if r_0^* is chosen to be a turning point of the geodesic (when such exists) (these initial data are inexact because the acceleration of the geodesic particle at t_0^* is not the one of a static particle, although its position and velocity are), or—for a marginally bounded particle (with $E = 1$)—if r_0^* is taken large enough. The difference between the actual initial field and the static initial data results in the occurrence of spurious waves superposed on the actual field; however, one may expect such waves to quickly die off, unveiling the intrinsic behavior of the field. Numerical experiments showed that this is indeed the case: The spurious waves were found to decay fast in all cases examined (see Fig. 2, e.g., for $r_0^* = 40M$). For a marginally bounded particle it has been confirmed that the field left after the spurious waves decay becomes independent of r_0^* —indicating that one indeed extracts the actual physical behavior. (In addition, we found that the larger r_0^* , the smaller the amplitude of the spurious waves, and the quicker they decay.)

To construct the difference scheme for the numerical integration we use a method similar to that applied by Lousto and Price in Ref. [14]. We integrate the field equation (4) over the unit cell shown in Fig. 1, which is centered at v, u and whose sides are of length $2h$. Let $\psi_1 \equiv \psi^\ell(v - h, u - h)$, $\psi_2 \equiv \psi^\ell(v - h, u + h)$, $\psi_3 \equiv \psi^\ell(v + h, u - h)$, and $\psi_4 \equiv \psi^\ell(v + h, u + h)$, and

suppose that ψ_1 , ψ_2 , and ψ_3 are already known, and we wish to calculate ψ_4 . Integration over the $\psi_{,uv}^\ell$ term in Eq. (4) yields (exactly) $\psi_1 - \psi_2 - \psi_3 + \psi_4$. Integration over the potential term yields $(\psi_1 + \psi_4)[1 + h^2 V^\ell(r)] - (\psi_2 + \psi_3)[1 - h^2 V^\ell(r)] + O(h^3)$. (Note that because ψ^ℓ is continuous across the worldline, the integration of the potential term here is much simpler than in [14], where the metric perturbations were studied using the Moncrief gauge, in which the wave function suffers a discontinuity across the worldline.) Finally, integrating over the source S (which is most easily done by transforming to the r, t coordinates, recalling that $dv du = 2F^{-1} dr dt$), we obtain $Z \equiv \int S dv du = 0$ if the worldline does not cross the cell, or, if it does,

$$Z = E^{-1} [k(t_{\text{out}}) - k(t_{\text{in}})] (t_{\text{out}} - t_{\text{in}}) + O(h^3). \quad (10)$$

Here, $k(t) \equiv F[r_p(t)]/r_p(t)$, and t_{in} (t_{out}) is the t value where the worldline enters (leaves) the cell. We can now extract the desired quantity ψ_4 . To $O(h^2)$ we find

$$\psi_4 = -\psi_1 + [1 - 2h^2 V^\ell(r)] (\psi_2 + \psi_3) + Z. \quad (11)$$

Our code, which is second-order convergent, evolves the scalar field in a straightforward marching. At each grid cell, the code does the following: (i) it decides whether or not the given worldline crosses the cell; (ii) if the worldline crosses the cell, it determines the point where it leaves it and calculates t_{out} (given t_{in}) to $O(h^2)$; (iii) it uses Eq. (11) to calculate the field ψ^ℓ at the cell's upper point; and (iv) at grid cells containing a section of the worldline, it constructs the quantities $f_{r^*}^\ell$ and f_t^ℓ by appropriately extrapolating the field gradients along the worldline (based on the already-derived values of the field at a few neighboring grid points).

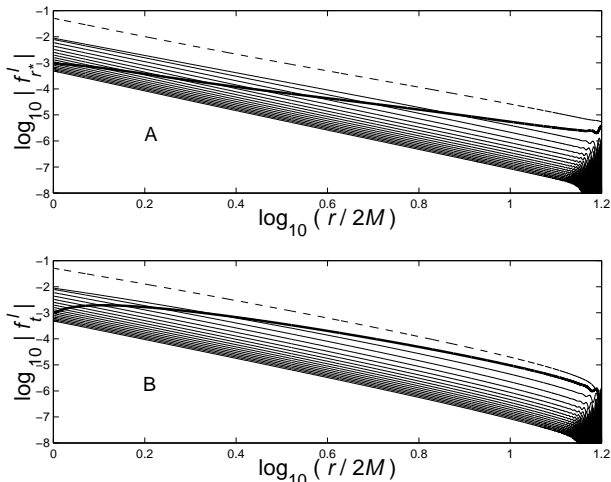


FIG. 2. The individual modes of the regularized RR force for a particle released from rest from $r_0^* = 40M$ as a function of r/M . Shown are the first 18 modes ($\ell = 0..17$). The monopole ($\ell = 0$) modes are displayed by dashed lines, and the dipole ($\ell = 1$) modes by thick lines. Except for the $\ell = 0, 1$ modes, the modes' amplitudes decrease monotonically with ℓ . Top panel (A): $f_{r^*}^\ell$. Bottom panel (B): f_t^ℓ .

We next present our results for a particle released from rest at $r_0^* = 40M$ (similar results are obtained also for other values of r_0^* and for the marginally-bound case). Figure 2 displays the behavior of the $f_{r^*}^\ell$ (2A) and f_t^ℓ (2B) components of the RR force. The $\ell = 0$ components are everywhere negative, whereas all the other modes ($\ell \geq 1$) are everywhere positive. Figure 2 also shows the decay of the spurious waves. Clearly, for values of r smaller than $25M$ they are already too small to be noticed.

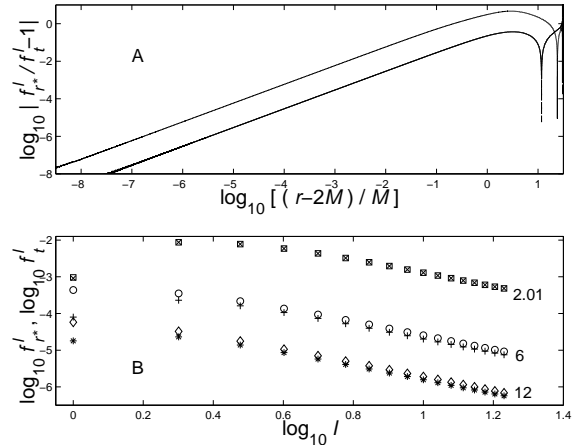


FIG. 3. Top panel (A): The relative difference $(f_{r^*}^\ell / f_t^\ell) - 1$ for $\ell = 0$ (upper) and $\ell = 1$ (lower) as functions of $(r - 2M)/M$. Bottom panel (B): The behavior of the individual modes as a function of the mode number ℓ for different values of r . Shown are $f_{r^*}^\ell$ for $r = 12M$ (*), $r = 6M$ (+), and $r = 2.01M$ (x), and f_t^ℓ for $r = 12M$ (\diamond), $r = 6M$ (o), and $r = 2.01M$ (\square).

Three properties of the behavior of the individual modes are particularly interesting: First, the dipole ($\ell = 1$) modes behave differently than the other modes, and the closer to the BH, the less important they are. Second, the relative importance of the higher modes increases approaching the BH. This will require care in the evaluation of the remainder of the series when we sum over all modes (see below). Third, as we approach the BH $f_{r^*}^\ell \rightarrow f_t^\ell$. This latter property is obvious from the following consideration: The covariant components f_v^ℓ and f_u^ℓ [where U is the outgoing Kruskal coordinate, satisfying $U \propto \exp(-u/4M)$ near the EH] assume finite values at the EH itself, as v and U are regular coordinates at the EH. Consequently, f_u^ℓ vanishes exponentially with u approaching the EH, yielding $f_t^\ell = f_v^\ell + f_u^\ell \rightarrow f_v^\ell$ and $f_{r^*}^\ell = f_v^\ell - f_u^\ell \rightarrow f_v^\ell$ as we approach the EH. Thus, $f_{r^*}^\ell \rightarrow f_t^\ell$. This is, in fact, a result of spatial gradients becoming comparable to temporal gradients near the EH. This behavior is shown in Figure 3(A) for two modes ($\ell = 0, 1$), but similar behavior is found also for all the other modes. Figure 3(B) displays the behavior of the modes as a function of the mode number ℓ , for various values of r . The individual modes behave like ℓ^{-2} for large values of ℓ . Note, that the closer the particle to the

BH, the later the asymptotic ℓ^{-2} behavior starts. Most importantly, the detailed behavior of the modes confirms the expressions for the analytically-derived regularization parameters [7,8].

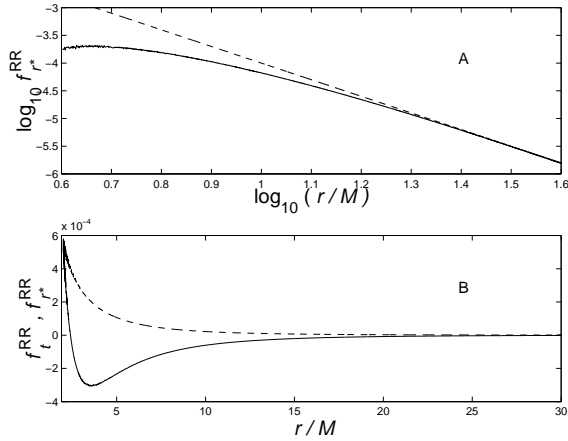


FIG. 4. The full RR force as a function of r . Top panel (A): $f_{r^*}^{\text{RR}}$ for a marginally-bound worldline (solid line) and the curve $-0.1 \times (r/M)^{-3}$ (dashed line). Bottom panel (B): Free fall from rest starting from $r_0^* = 40M$. Dashed line: f_t^{RR} . Solid line: $f_{r^*}^{\text{RR}}$.

Next, we sum over all modes to find the total RR force. As noted above, the relative importance of the higher modes increases as we approach the horizon. This causes two problems: (i) it is crucial to include an accurate approximation of the remainder of the series due to our computation of only a finite number of modes, and (ii) the noise contribution from the ℓ -mode to the overall force increases with ℓ . The ℓ^{-2} behavior of the modes indicates that we can sum over the modes and calculate the remainder as was done in Ref. [10]. Specifically, the full RR force is

$$f_\alpha^{\text{RR}} = \sum_{n=0}^{\ell} f_\alpha^{n(\text{reg})} + \mathcal{R}_\alpha^{\ell+1}, \quad (12)$$

where the remainder can be approximated by $\mathcal{R}_\mu^{\ell+1} \approx \ell^2 f_\mu^{\ell \text{ tail}} \psi^{(1)}(\ell+1)$. Here, $f_\alpha^{n(\text{reg})}$ is the regularized ℓ -mode of the force, and $\psi^{(1)}(x) \approx x^{-1} + x^{-2}/2 + x^{-3}/6 + O(x^{-5})$ is the trigamma function. As we sum the series only up to $\ell = 17$, this approximation for $\mathcal{R}_\mu^{\ell+1}$ guarantees accuracy of 7×10^{-4} (we neglect here the contribution to $\mathcal{R}_\mu^{\ell+1}$ from terms which scale like ℓ^{-3}). Obviously, approaching the EH $f_{r^*} \rightarrow f_t$ (as each of the individual modes does). Figure 4 shows the full RR force as a function of r for two cases: Fig. 4(A) shows $f_{r^*}^{\text{RR}}$ for a marginally-bound trajectory ($E = 1$). At large distances this force behaves like $f_{r^*}^{\text{RR}} \approx -(G/c^2)\beta q^2 M/r^3$. The exponent of r is found here to a 1% accuracy, and we find the parameter $\beta = (1.00 \pm 0.15) \times 10^{-1}$. Figure 4(B) shows the case of fall from rest, starting from $r_0^* = 40M$. At large values of r both components of the

force vanish, in accord with the vanishing of the force for a static scalar charge. The covariant t component, f_t^{RR} , is everywhere positive and increases monotonically approaching the BH. This is a consequence of the particle losing energy by radiating, part of which escapes to infinity, and the rest being captured by the BH. The covariant r^* component, $f_{r^*}^{\text{RR}}$, is attractive at large distances. However, near the peak of the effective potential barrier (near $r^* \approx 0$) its behavior changes, and near the EH it approaches the value of f_t^{RR} , as expected. Note that both components arrive at the EH at a bounded value. Because f_t^{RR} is expected to be positive (the particle only loses energy by radiating), we infer that $f_{r^*}^{\text{RR}}$ would also be positive approaching the EH, under very general conditions. In particular, if this behavior persists also for charged BHs, and for an electrically-charged particle, then the properly-defined covariant spatial-component of the RR force at the EH would be repulsive. If this is indeed the case, then the RR force acts to reduce the parameter space for which a nearly-extreme spherical charged BH can be overcharged [15]. The question of whether cosmic censorship for that case is saved by RR effects, however, awaits further considerations.

We thank Amos Ori, Lee Lindblom, and Kip Thorne for discussions. LMB wishes to thank the Technion Institute of Theoretical Physics, where part of this research was done, for hospitality. At Caltech this research was supported by NSF grants AST-9731698 and PHY-9900776 and by NASA grant NAG5-6840.

-
- [1] See, e.g., E. Poisson and S. W. Leonard, Phys. Rev. D **56**, 4789 (1997) and references cited therein.
 - [2] S. A. Hughes, Phys. Rev. D **61**, 084004 (2000).
 - [3] T. C. Quinn and R. M. Wald, Phys. Rev. D **56**, 3381 (1997).
 - [4] Y. Mino, M. Sasaki, and T. Tanaka, Phys. Rev. D **55**, 3457 (1997).
 - [5] A. Ori, Phys. Lett. A **202**, 347 (1995); Phys. Rev. D **55**, 3444 (1997).
 - [6] A. Ori, unpublished.
 - [7] L. Barack and A. Ori, Phys. Rev. D **61**, 061502(R) (2000).
 - [8] L. Barack, Phys. Rev. D (in press) (gr-qc/0005042).
 - [9] L. M. Burko, Class. Quantum Grav. **17**, 227 (2000).
 - [10] L. M. Burko, Phys. Rev. Lett. **84**, 4529 (2000).
 - [11] L. M. Burko, Am. J. Phys. **68**, 456 (2000).
 - [12] C. O. Lousto, Phys. Rev. Lett. **84**, 5251 (2000).
 - [13] L. M. Burko, in *Gravitational Waves: Third Edoardo Amaldi conference*, edited by S. Meshkov (AIP, New York, 2000) (gr-qc/9911089)
 - [14] C. O. Lousto and R. H. Price, Phys. Rev. D **56**, 6439 (1997).
 - [15] V. E. Hubeny, Phys. Rev. D **59**, 064013 (1999).